Available online at www.sciencedirect.com

ScienceDirect

IFAC Papers Online CONFERENCE PAPER ARCHIVE

IFAC PapersOnLine 50-1 (2017) 966–971

Anti-Jerk Control of a Parallel Hybrid Electrified Vehicle with Dead Time

Truc Pham [*,**] **Robert Seifried** [*] **Christian Scholz** [**]

[*] *Institute of Mechanics and Ocean Engineering, Hamburg University of Technology, 21073 Hamburg, Germany (e-mail: robert.seifried@tuhh.de).*

[**] *Porsche Research and Development Centre, 71287 Weissach, Germany (e-mail: {hong_truc.pham, christian.scholz}@porsche.de)*

Abstract: Anti-jerk controller are essential for drive comfort during load-changes, since they reduce undesired driveline oscillations. Hybrid electrified vehicles enable greater degree of freedom to control these oscillations due to the two actuators, namely internal combustion engine and electric machine. At the same time the more complex communication structure of electronic control units in a hybrid electrified vehicle inserts more time delay in the system, which can cause instability in driveline oscillation control. This paper analysis the effect of dead time on a parallel hybrid electrified driveline model with proportional feedback controller and present a feedforward and feedback strategy with dead time compensation. Simulation results of the proposed approach show good step-response behavior and robustness against dead time.

Keywords: driveline control, hybrid electrified vehicle, dead time, anti-jerk, three-mass model

1. INTRODUCTION

In recent years, hybrid electrified vehicles attracted much attention. It is becoming increasingly important to develop efficient and simultaneously high-performance vehicles as addressed in Emadi et al. (2008). Parallel hybrid electrified vehicles provide additional degrees of freedom to drive a car. Particularly, parallel hybrid electrified vehicles allow to drive a car in pure internal combustion engine (ICE) mode, electric machine (EM) mode or in a joint mode of ICE and EM. This additional degree of freedom can be used to confront different issues in driveline control.

Much study focus on control design to reduce driveline oscillations. Especially, driveline jerking plays a key role in research. Jerking may occur by rapid driving maneuvers, for instance when the driver quickly press the accelerator pedal, see Grotjahn et al. (2006). In Templin and Egardt (2009), Joachim et al. (2014) and Pham et al. (2016) controllers are designed to reduce driveline oscillations, however only for conventional powertrains. In Angeringer et al. (2012) a sliding mode controller is used to control the drive shaft torque of an electrically driven vehicle. Control design for parallel hybrid electrified vehicles to reduce cyclic irregularity of the ICE is discussed in Vadamalu and Beidl (2016). All this work is based on a two-mass control model of the driveline. However, to control driveline oscillations of a parallel hybrid electrified vehicles it is advantageous to use a three-mass control model including the masses of ICE, EM, and vehicle.

Another important aspect in driveline control is that the number of electric control units (ECU) in a vehicle increases, see Bayindir et al. (2011), and therefore the number of options where to implement the control law. This decision depends for instance on the torque split strategy between ICE and EM.

Figure 1 illustrates the interplay between ICE ECU, EM ECU and driving dynamics ECU in a parallel hybrid electrified vehicle. Between ICE ECU and driving dynamics ECU exists a time delay of τ_1, between ICE ECU and EM ECU exists a communication delay of τ_2 and between ICE EM and driving dynamics ECU exists a communication delay of τ_3. These dead times may lead to measurement delay and actuator delay in the control loop.

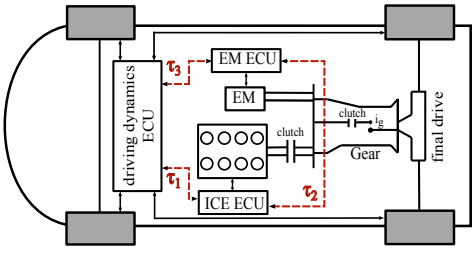

Fig. 1. ECUs in a rear driven parallel hybrid electrified vehicles with communication delays τ_1, τ_2, and τ_3.

Depending on where the driveline controller is implemented, time delays play an important role regarding to stability and performance of the controlled system. These circumstances should be considered in anti-jerk control design to reduce driveline oscillation.

In this paper we focus on anti-jerk control during ICE load changes. A three-mass control model as the basis for feedforward control design and dead time compensation is presented. Analysis of the effect of dead time on the three-mass system with proportional feedback controller is shown. The feedforward control strategy inverts the driveline model by differentially flatness theory and is

10.1016/j.ifacol.2017.08.172

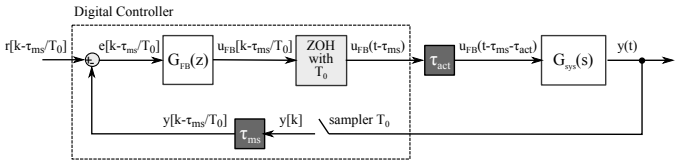

Fig. 2. Digital feedback control loop with actuator dead time τ_{act}, measurement dead time τ_{ms} and control unit sampling time T_0.

applied to the ICE to prevent jerking during ICE load changes. The feedback control strategy with dead time compensation is applied to the EM. An observer with state extension is used to compensate measurement dead time, while state prediction is used to compensate actuator dead time. The goal of the control strategy is that it is easy to implement, ensure system performance and gives robustness to dead time. The approach is evaluated through simulation studies.

The paper is organized as follows. Section 2 provides an analysis of dead time in the control system, description of a detailed parallel hybrid electrified vehicles model and of the three-mass control model. In Section 3 the effect of dead time in the control loop is presented and a feedforward controller as well as a feedback controller with dead time compensation are derived. Section 4 contains simulation results for the presented control approach and Section 5 concludes the paper.

2. MODELING OF A PARALLEL HYBRID DRIVELINE WITH DEAD TIME

In this section the analyzed dead time scenario in a parallel hybrid electrified driveline is presented. Then a detailed powertrain model of a parallel hybrid electrified vehicle is described. This model is then used to derive a reduced three-mass control model and for simulation study.

2.1 Sources of Dead Time in the Control Loop

In parallel hybrid electrified vehicles an energy management strategy is required, since the torque has to be split between ICE and EM. This strategy has to be implemented in an ECU. Thereby, it is preferable that the control strategy for ICE as well as EM is calculated at the same place as the energy management strategy. In this work, the control strategy is implemented in the ICE ECU. A feedforward control strategy is derived for the ICE and a feedback controller is implemented to reduce driveline oscillations using the EM. The feedback controller uses delayed measurements, sent by the driving dynamics ECU. Thus as shown in Figure 2, the communication dead time τ_1 in Figure 1 corresponds to measurement delay τ_{ms}. The calculated input u_{ctrl} for the EM is delayed by the communication between ICE ECU and EM ECU, such that communication dead time τ_2 in Figure 1 corresponds to actuator dead time u_{act} in Figure 2.

2.2 Detailed Model of a Parallel Hybrid Electrified Driveline

For driveline control design, a powertrain is generally modeled as a chain of lumped inertias coupled by spring and damper elements, see Eriksson and Nielsen (2014).

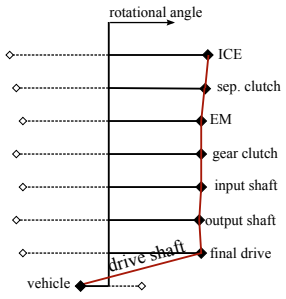

Fig. 3. 1st eigenmode

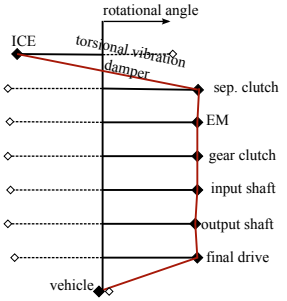

Fig. 4. 2nd eigenmode

As discussed in Jarczyk et al. (2009), the particularity of a parallel hybrid electrified vehicle driveline is that two system inputs u_{ICE} and u_{EM} can act on the system, see Figure 1. Moreover, two heavier inertias are placed in the front part of the vehicle and the system includes a separation clutch and a clutch for gear shifting. The separation clutch can separate the ICE from the remaining driveline, such that it is possible to drive the parallel hybrid electrified vehicle in pure ICE mode, pure electric mode or in hybrid mode.

In total the detailed model has 8 degrees of freedom. Coupling elements are represented by stiffness and damping functions depending on the phase and speed difference, respectively and can be nonlinear.

Using modal analysis the frequencies of the system and its eigenforms for each gear can be detected. Figure 3 and Figure 4 show the first and second eigenmode of a parallel hybrid electrified vehicle model with inertias ICE, separation clutch, EM, gear clutch, input shaft, output shaft, final drive, and vehicle. The relative rotational angle of each inertia is depicted on the x-axis, such that the deflection shape is illustrated for the particular eigenfrequency. In the first eigenmode the drive shaft is responsible for the counter-phase vibration between ICE to final drive and wheels, and in the second eigenmode the torsional vibration damper is responsible for the counter-phase vibration between ICE and separation clutch to final drive. Therefore drive shaft and torsional vibration damper significantly influence the dynamics of the driveline in the first and second mode. The typical eigenfrequency of the first eigenmode is between 1 and 8 Hz depending on the chosen gear and the frequency of the second eigenmode is typically in the range between 20 and 50 Hz, mainly depending on the torsional vibration damper characteristic.

2.3 Control Model of a Parallel Hybrid Driveline

For controller design a simplified driveline model is derived. Using the knowledge from the previous eigenmode and eigenfrequency analysis of the detailed system, a three mass model as depicted in Figure 5 is deduced.

The system parameters can be identified using the detailed powertrain model or measurements. If vehicle data is available, the following equations provide good parameter estimation:

$$J_1 = J_{ICE}, \quad J_2 = J_{EM}, \quad J_3 = m_{veh} r_w^2,$$
$$c_1 = c_{td}, \quad c_2 = c_{ds}, \quad d_1 = d_{td}, \quad d_2 = d_{ds}$$

with m_{veh} as the vehicle mass, r_w as the tire radius, c_{td} and d_{td} as the stiffness and damping constant of the

torsional vibration damper, and c_{ds} and d_{ds} as the stiffness and damping constant of the drive shaft. The moments of inertia of ICE, EM and vehicle are denoted as J_1, J_2 and J_3. The ICE torque input is referred to u_{ICE} and the EM torque input to u_{EM}. Moreover, φ_1 and ω_1 denotes the rotational angle and speed of the ICE, φ_2 and ω_2 the rotational angle and speed of the EM and s_{veh} and v_{veh} the displacement and speed of the vehicle.

The system state is defined as $x = [\,\Delta\varphi_1\ \Delta\varphi_2\ \omega_1\ \omega_2\ \omega_3\,]^T$ with $\Delta\varphi_1 = \varphi_1 - \varphi_2$ and $\Delta\varphi_2 = \frac{\varphi_2}{i_g} - s_{veh} r_w$ with gear ratio i_g and ω_1, ω_2, and ω_3 as rotational speed with $\omega_3 = v_{veh} r_w$. The system equations are then

$$\begin{aligned}
\Delta\dot{\varphi}_1 &= \omega_1 - \omega_2 \\
\Delta\dot{\varphi}_2 &= \frac{\omega_2}{i_g} - \omega_3 \\
\dot{\omega}_1 &= \frac{1}{J_1}\left(u_{ICE} - c_1\Delta\varphi_1 - d_1\left(\omega_1 - \omega_2\right)\right) \\
\dot{\omega}_2 &= \frac{1}{J_2}\left(u_{EM} + c_1\Delta\varphi_1 + d_1\Delta\omega_1\right) \\
&\quad - \left(\frac{1}{J_2 i_g}\left(c_2\Delta\varphi_2 + d_2\left(\frac{\omega_2}{i_g} - \omega_3\right)\right)\right) \\
\dot{\omega}_3 &= \frac{1}{J_3}\left(c_2\Delta\varphi_2 + d_2\left(\frac{\omega_2}{i_g} - \omega_3\right)\right).
\end{aligned} \tag{1}$$

This 5^{th} order model (1) can be reduced to a 4^{th} order model by introducing $x = [\,\Delta\varphi_1\ \Delta\varphi_2\ \Delta\omega_1\ \Delta\omega_2\,]^T$ as new state, with $\Delta\omega_1 = \omega_1 - \omega_2$, and $\Delta\omega_2 = \frac{\omega_2}{i_g} - v_{veh} r_w$. This leads to

$$\dot{x} = \underbrace{\begin{bmatrix} 0 & 0 & 1 & 0 \\ 0 & 0 & 0 & 1 \\ -c_1\alpha_1 & \frac{c_2}{J_2 i_g} & -d_1\alpha_1 & \frac{d_2}{J_2 i_g} \\ \frac{c_1}{J_2 i_g} & -c_2\alpha_2 & \frac{d_1}{J_2 i_g} & -d_2\alpha_2 \end{bmatrix}}_{A_c} x + \underbrace{\begin{bmatrix} 0 & 0 \\ 0 & 0 \\ \frac{1}{J_1} & -\frac{1}{J_2} \\ 0 & \frac{1}{J_2 i_g} \end{bmatrix}}_{B_c} \begin{bmatrix} u_{ICE} \\ u_{EM} \end{bmatrix}. \tag{2}$$

with $\alpha_1 = \frac{J_1 + J_2}{J_1 J_2}$ and $\alpha_2 = \frac{J_2 i_g^2 + J_3}{J_2 J_3 i_g^2}$.

3. CONTROL STRATEGY

The first part of this section analysis the closed loop behavior of control model (2), when a proportional feedback controller is used. It is shown that there is a trade-off between performance and robustness against dead time. In the second part of this section, a model based feedforward controller is derived to enhance the performance. In the third part of this section a feedback controller is discussed. The feedback controller is an extension of the analyzed proportional controller. The extension bases on a state observer and state predictor to compensate dead time.

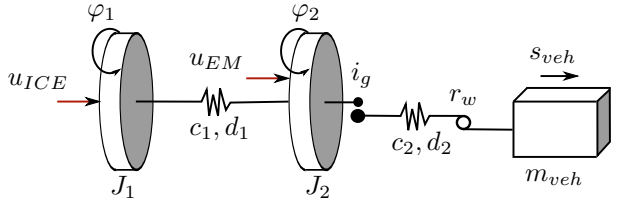

Fig. 5. Three mass control model

In the last part, the overall control strategy is presented. The strategy consists of a digital control loop with the derived feedforward controller and proportional feedback controller with dead time compensation.

3.1 System Analysis of a Proportional Closed Loop System with Dead Time

Measurement dead time τ_{ms}, actuator dead time τ_{act} and sampling time T_0 influence the stability of the closed loop system as depicted in Figure 2. Measurement and actuator dead time mainly occur due to communication delay between control units. Sampling dead time occurs based on a digital-to-analog converter as zero-order hold. The driveline is represented by the continuous system $G_{sys}(s)$, but a controller has to be realized discrete, such that digital-to-analog converter and analog-to-digital sampler are necessary.

The digital-to-analog converter delays the closed loop system by half of the sampling time T_0, which can be seen, if the transfer function of a zero order hold is considered as discussed in Franklin et al. (1997). Thus, the total dead time in the control loop, shown in Figure 2 is

$$\tau_{total} = \tau_{ms} + \tau_{act} + \frac{T_0}{2}.$$

The system output is defined as the rotational speed difference between electric machine ω_2 and wheels ω_3 with consideration of the gear ratio and reads

$$y = \frac{\omega_2}{i_g} - \omega_3 = \underbrace{[\,0\ 0\ 0\ 1\,]}_{C_c} x. \tag{3}$$

The following continuous feedback controller is applied to system (2) without dead time

$$u_{FB}(t) = K\left[r\left(t\right) - y\left(t\right)\right], \tag{4}$$

with $K \in \mathbb{R} > 0$ and $r(t)$ as the reference value. Analysis of the closed loop eigenvalues of the system without dead time shows that the damping increases for increasing control gain K.

In order to analyze the effect of dead time, the delay-margin of the open loop system is significant for closed loop stability.

Definition 1. (Normey-Rico and Camacho (2007)). The *delay margin* is characterized by the minimum time delay $\tau_{margin} > 0$ such that the closed-loop system becomes unstable. It can be calculated by the phase margin ϕ_r and the crossover frequency ω_0 of the open loop system as

$$\tau_{margin} = \frac{\phi_r}{\omega_0}.$$

The bode plot in Figure 6 demonstrates that for increasing control gain K the phase margin decreases and the crossover frequency increases. Hence, the delay margin of the parallel hybrid electrified driveline system (2) decreases for greater control gain and the system can become unstable.

In summary, the digital control loop of a parallel hybrid electrified vehicle contains of high dead times. Increasing the control gain would lead to better system performance, if there is no dead time, but for dead time systems it may degrade the delay margin. This results in a trade-off between performance and adequate delay margin.

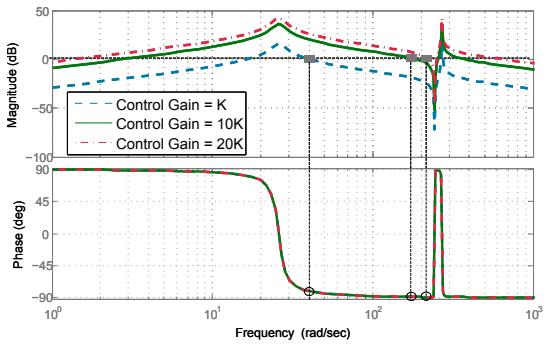

Fig. 6. Bode diagram with various control gains.

3.2 Model-based Feedforward Controller

A feedforward controller is designed to increase the performance without affecting the system's stability and degrading its robustness. Differential flatness is used to derive such a feedforward controller.

In the general nonlinear case, a system is said to be *differentially flat*, if and only if there exists a flat output, such that system state, input, and output can be fully described by the flat output and its derivatives, see M. Fliess (1995). Thus, the system can be analytically inverted.

In the particular case of linear systems the property differentially flatness is equivalent to controllability. The flat output z can be constructed by the last row of the Kalman controllability matrix as discussed in Zeitz (2010),

$$z = \lambda^T x,$$

with

$$\lambda^T = e^T P^{-1}.$$

Hence, P^{-1} is defined as the inverse Kalman controllability matrix and it is

$$e^T = [\,0\ 0\ \dots\ 0\ \beta\,] \in \mathbb{R}^n$$

with n as the system order. The value β can be chosen as a constant unequal to zero.

Then, the feedforward control law, as shown in Zeitz (2010), reads for an n^{th} order system

$$u_{FW}(t) = \frac{1}{\beta}\left(z_{ref}^{(n)}(t) + \kappa \begin{bmatrix} z_{ref}(t) \\ \dot{z}_{ref}(t) \\ \ddot{z}_{ref}(t) \\ \vdots \\ z_{ref}^{(n-1)}(t) \end{bmatrix} \right) \tag{5}$$

with

$$\kappa = -\lambda^T A^n T^{-1}, \tag{6}$$

where A is defined as the system matrix and T as the transformation matrix

$$x^* = \begin{bmatrix} z \\ \dot{z} \\ \ddot{z} \\ \vdots \\ z^{(n-1)} \end{bmatrix} = \underbrace{\begin{bmatrix} \lambda^T \\ \lambda^T A \\ \lambda^T A^2 \\ \vdots \\ \lambda^T A^{n-1} \end{bmatrix}}_{=:T} x. \tag{7}$$

For the driveline system (2) with input u_{ICE} the flat output z can be constructed by

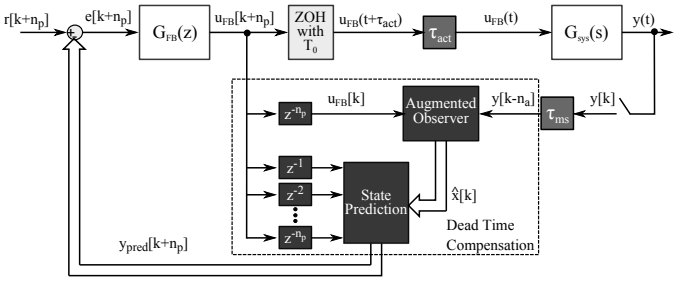

Fig. 7. Digital control loop to compensate measurement dead time τ_{ms} and actuator dead time τ_{act} via EM.

$$\lambda^T = [\, J_1 d_1^2,\ J_1 J_2 i_g (c_1 - d_1 d_2 \alpha_2),\ 0,\ -J_1 J_2 d_1 i_g \,] \tag{8}$$

and chosen

$$\beta = -c_1 d_1 d_2 \alpha_2 + c_2 d_1^2 \alpha_2 + c_1^2. \tag{9}$$

Hence, the flat output is described as a function of the system states $\Delta\varphi_1$, $\Delta\varphi_2$ and $\Delta\omega_2$ by

$$z = J_1 d_1^2 \Delta\varphi_1 + J_1 J_2 i_g (c_1 - d_1 d_2 \alpha_2)\Delta\varphi_2 - J_1 J_2 d_1 i_g \Delta\omega_2.$$

Using (8), (9), the feedforward control law (5) for the driveline system (2) with input u_{ICE} is given.

A desired trajectory $z_{ref}(t)$ with defined n derivatives has to be planned for control law (5) to steer from one equilibrium to another. The start and end point of the desired trajectory are determined by the equilibrium points of the system (2). The transition time and the type of the trajectory are available design parameters. For instance a polynomial trajectory can be applied.

3.3 Dead Time Compensation for Feedback Controller

The feedback controller for input u_{EM}, which is derived in this part, will be implemented discrete, therefore the driveline system (2) is discretized for control design. The continuous system is sampled and the input is modeled as zero-order hold

$$\begin{aligned} x_{k+1} &= A_d x_k + B_d u_k, \\ y_k &= C_d x_k \end{aligned} \tag{10}$$

with

$$A_d = e^{A_c T_0}, \quad B_d = \int_{\upsilon=0}^{\upsilon=T_0} e^{A_c \upsilon} d\upsilon B_c$$

$$C_d = [\,0\ 0\ 0\ 1\,]$$

and discrete state vector

$$x_k = [\,\Delta\varphi_{1,k}\ \ \Delta\varphi_{2,k}\ \ \Delta\omega_{1,k}\ \ \Delta\omega_{2,k}\,]^T.$$

As shown in Figure 2 the control loop consists of measurement and actuator dead time. To compensate measurement dead time a Luenberger observer is designed for an augmented system, which represent the delay as system state, see Franklin et al. (1997). The second component of the controller predicts future states to compensate actuator dead time as applied in Vadamalu and Beidl (2016). The overall feedback control structure is depicted in Figure 7.

Observer Design of Augmented System
Measurement dead time τ_{ms} is explicitly considered in an augmented system of (10) with $n_a = \frac{\tau_{ms}}{T_0}$ additional states and sampling time T_0. The augmented state is then

$$x_{k,a} = \left[\, \Delta\varphi_{1,k},\ \Delta\varphi_{2,k},\ \Delta\omega_{1,k},\ \Delta\omega_{2,k},\ \Delta\omega_{2,k-1},\ \dots,\ \Delta\omega_{2,k-n_a} \,\right]^T$$

and the augmented system is

$$A_{d,a} = \begin{bmatrix} A_d(1,1) & \dots & A_d(1,4) & 0 & \dots & 0 & 0 \\ \vdots & & \vdots & & 0 \dots 0 & & 0 \\ \vdots & & \vdots & & & & \\ A_d(4,1) & \dots & A_d(4,4) & 0 & \dots & 0 & 0 \\ 0 & 0 & 1 & 0 & \dots & 0 & 0 \\ 0 & 0 & 0 & 1 & \dots & 0 & 0 \\ \vdots & & & & \ddots & & \vdots \\ 0 & 0 & 0 & 0 & \dots & 1 & 0 \end{bmatrix} \in \mathbb{R}^{(n+n_a)\times(n+n_a)},$$

$$B_{d,a} = \begin{bmatrix} B_d(1,1) & B_d(1,2) \\ \vdots & \vdots \\ B_d(n,1) & B_d(n,2) \\ 0 & 0 \\ \vdots & \vdots \\ 0 & 0 \end{bmatrix},$$

$$y_{k,a} = \Delta\omega_{2,k-n_a} = \underbrace{\begin{bmatrix} 0 & 0 & \dots & 0 & 1 \end{bmatrix}}_{C_{d,a}\in\mathbb{R}^{n+n_a}} x_{k,a}, \tag{11}$$

with $A_d(i,j)$ and $B_d(i,j)$ as the j^{th}-element in the i^{th}-row of the discrete system matrix A_d and input matrix B_d, respectively.

A Luenberger observer

$$\dot{\hat{x}}_{k,a} = (A_{d,a} - LC_{d,a})\,\hat{x}_k + [\,B_{d,a}\;\; L\,] \begin{bmatrix} u_{k,a} \\ y_{k,a} \end{bmatrix} \tag{12}$$

with gain $L \in \mathbb{R}^{n+n_a}$ can be designed for the augmented system (11), such that the poles of the observer error dynamics $(A_{d,a} - LC_{d,a})$ are faster than the poles of the closed loop system with controller (4). Subsequently, the predicted state without measurement delay

$$\hat{x}_k = [\,\Delta\hat{\varphi}_{1,k},\; \Delta\hat{\varphi}_{2,k},\; \Delta\hat{\omega}_{1,k},\; \Delta\hat{\omega}_{2,k}\,]$$

is applied for state prediction.

State Prediction

The state predictor calculates $n_p = \frac{\tau_{act}}{T_0}$ future states to compensate actuator dead time τ_{act}. The approach is recursive and model-based. Therefore, to predict n_p steps into the future, the following law has to be calculated

$$x_{k+n_p} = A_d^{n_p} x_k + \sum_{i=0}^{n_p-1} A_d^i B_d u_{k+n_p-1-i}. \tag{13}$$

Then, the extended discrete feedback controller with predicted output y_{k+n_p} is

$$u_{FB,k+n_p} = K\left[r_{k+n_p} - y_{k+n_p}\right]. \tag{14}$$

3.4 Overall Control Structure

The overall combined control structure shows Figure 8. Feedforward and feedback controller are implemented discrete. Feedforward control law (5) can be transformed to discrete implementation, if the reference trajectories are planned in discrete form $z[k], z'[k], \dots, z^{[n]}[k]$. As depicted in Figure 8 the reference $r\,[k+n_p]$ and therefore the feedforward control input $u_{FW,ICE}\,[k+n_p]$ have to be planned ahead to compensate the actuator dead time τ_{act} using the ICE, as discussed in Rudolph (2005). The

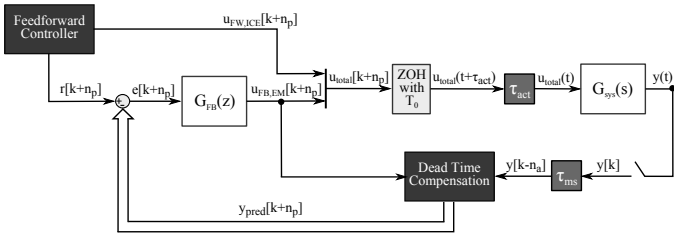

Fig. 8. Overall digital control loop with feedforward controller $u_{FW,ICE}$ and feedback controller $u_{FB,EM}$.

feedback controller $G_{FB}(z)$ regulates the predicted error $e\left[k + \frac{\tau_{act}}{T_{ctrl}}\right]$ to zero using the EM.

4. SIMULATION RESULTS

The proposed control strategy for systems with measurement and actuator dead time is evaluated on a detailed parallel hybrid electrified driveline simulation model via Matlab. Actuator and measurement dead time are set to $\tau_{act} = \tau_{ms} = 20\ ms$ and the control sample time is defined as $T_0 = 10\ ms$. Five strategies are compared by application to the detailed simulation model. Simulation parameters and numerical values are not provided due to reasons of confidentiality, but qualitative statements are given.

In $V1 - V4$ the ICE input is a filtered ramp, see Figure 9 and in $V5$ the input is derived by the proposed feedforward controller (5), see Figure 10. In all strategies the EM control method differ:

V1 no controller
V2 proportional feedback controller (4) with gain K
V3 proportional feedback controller (4) with half gain $0.5K$
V4 proportional feedback controller (4) with gain K and compensation methods (12) and (13)
V5 proportional feedback controller (4) with control gain K, compensation methods (12) and (13), feedforward controller (5) and dynamic reference

Figure 9 compares strategies $V1 - V4$. As can be seen in the first sub-figure, no feedforward controller is applied to the ICE and the control reference r is specified to zero. As shown in the signals of $V1$, the system is induced by the step input of the ICE torque. The system is not controlled and the vehicle longitudinal acceleration oscillates with highest amplitude and decays only slowly. The system

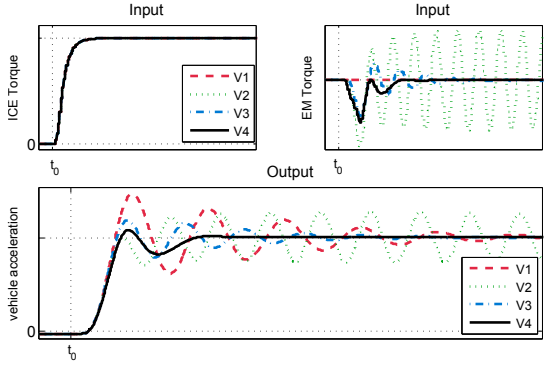

Fig. 9. Comparison of methods $V1 - V4$.

with method $V2$ become unstable due to the feedback controller and dead time in the control loop as seen by the increase of vibration amplitude of EM torque and of vehicle acceleration. When the control gain is halved as in method $V3$, the controlled system is no longer unstable, but the decay behavior is slow. In method $V4$ the proposed strategy with dead time compensation is applied. It shows no instability and the best system response with fast vibration amplitude decay.

Additionally to the control method $V4$, a feedforward controller as described in (5) is implemented in method $V5$. Therefore, the dynamic reference $r = \Delta\omega_{2,ref}$, planned by the flatness-based feedforward controller, is applied for the extended proportional controller.

Methods $V4, V5$ with dead time compensation are analyzed in Figure 10. Compared to method $V4$, where the ICE torque is just a filtered ramp, the ICE torque in $V5$ is based on the model-based feedforward control law (5). The specific shape is clearly recognizable. Further, the control torque applied in the EM of method $V5$ is negative as well as positive, which differs to the exclusively reducing control torque of method $V4$. As depicted in the third sub-figure the reference value $\Delta\omega_{2,ref}$ of method $V5$ is shaped as a peak and is not constantly zero as in method $V4$. The dynamic reference allows positive rotational speed $\Delta\omega_2$ for a specific period. Therefore, the control amplitude of method $V5$ is smaller. The last sub-figure shows that methods $V4$ and $V5$ have much better step response behavior than the uncontrolled version and method $V5$ shows even less vibration than $V4$.

The simulation results of method $V5$ demonstrate that the closed loop system is robust to dead time and provides very good system performance.

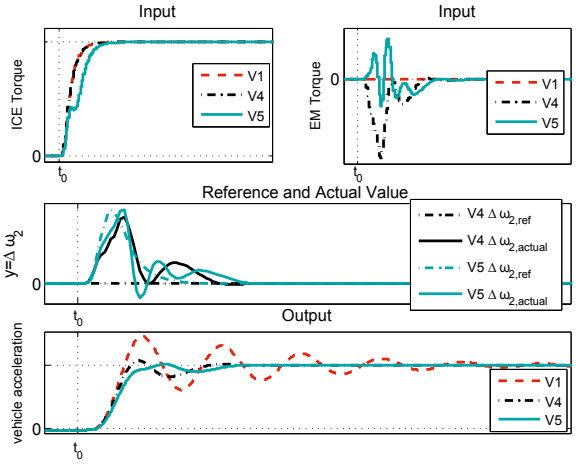

Fig. 10. Comparison of compensation methods $V4$ and $V5$.

5. CONCLUSION

The importance of incorporating dead time in driveline control design of parallel hybrid electrified vehicle was illustrated. A control method based on a three-mass model with feedforward and feedback controller was presented. The feedforward controller inverts the three-mass model and provides performance. The feedback controller compensates dead time by system augmentation and an observer, and state predictor. Simulation study on a detailed simulation model showed improved stability and performance. Future work will involve experimental validation.

REFERENCES

Angeringer, U., Horn, M., and Reichhartinger, M. (2012). Drive line control for electrically driven vehicles using generalized second order sliding modes. *IFAC Proceedings Volumes*, 45(30), 79 – 84.

Bayindir, K.C., Gzkck, M.A., and Teke, A. (2011). A comprehensive overview of hybrid electric vehicle: Powertrain configurations, powertrain control techniques and electronic control units. *Energy Conversion and Management*, 52(2), 1305 – 1313.

Emadi, A., Lee, Y.J., and Rajashekara, K. (2008). Power electronics and motor drives in electric, hybrid electric, and plug-in hybrid electric vehicles. *IEEE Transactions on Industrial Electronics*, 55(6), 2237–2245.

Eriksson, L. and Nielsen, L. (2014). *Modeling and Control of Engines and Drivelines*. Wiley.

Franklin, G.F., Workman, M.L., and Powell, D. (1997). *Digital Control of Dynamic Systems*. Addison-Wesley Longman Publishing Co., Inc., 3rd edition.

Grotjahn, M., Quernheim, L., and Zemke, S. (2006). Modelling and identification of car driveline dynamics for anti-jerk controller design. *Proceeding of IEEE International Conference on Mechatronics*, 131–136.

Jarczyk, J.C., Alt, B., Blath, J.P., Svaricek, F., and Schultalbers, M. (2009). Decoupling control for the speed synchronization task in the powertrain of a hybrid electric vehicle. *Proceeding of 2009 IEEE International Conference on Control and Automation*, 2154–2159.

Joachim, C., Reuss, H.C., and Horwath, J. (2014). An example for the use of adaptive methods in powertrain control of heavy duty vehicles. Application of torque control functions for optimized gear shifting. *Proceeding of Internationaler VDI-Kongress: Getriebe in Fahrzeugen*.

M. Fliess, J. Levine, P.R. (1995). Flatness and defect of nonlinear systems: Introductory theory and examples. *International Journal of Control*, 61, 1327–1361.

Normey-Rico, J.E. and Camacho, E. (2007). *Control of Dead-time Processes*. Springer-Verlag London, 1st edition.

Pham, T., Seifried, R., Hock, A., and Scholz, C. (2016). Nonlinear flatness-based control of driveline oscillations for a powertrain with backlash traversing. *Proceeding of 8th IFAC Symposium on Advances in Automotive Control*, 49(11), 749 – 755.

Rudolph, J. (2005). Flatness: A useful property also for systems with delays. *Automatisierungstechnik*, 53, 178–188.

Templin, P. and Egardt, B. (2009). An LQR torque compensator for driveline oscillation damping. *Proceeding of IEEE International Conference on Control Application (CCA)*, 352–356.

Vadamalu, R.S. and Beidl, C. (2016). MPC for active torsional vibration reduction of hybrid electric powertrains. *Proceeding of 8th IFAC Symposium on Advances in Automotive Control*, 49(11), 756 – 761.

Zeitz, M. (2010). Differential flatness: A useful method also for linear SISO systems. *at - Automatisierungstechnik*, 58(1), 5–13.